PROCEEDINGS OF SCIENCE

Data-driven method to quantify and correct the corner-clipping effect in segmented muon counters

J. de Jesús,[a,b,*] **J.M. Figueira,**[a] **F. Sánchez**[a] **and D. Veberič**[b]

[a] *Instituto de Tecnología y Detección en Astropartículas (CNEA, CONICET, UNSAM), Buenos Aires, Argentina*

[b] *Karlsruhe Institute of Technolgy (KIT), Institute for Astroparticle Physics, Karlsruhe, Germany*

E-mail: joaquin.dejesus@iteda.gob.ar

Segmented muon detectors, such as the Underground Muon Detector (UMD) of the Pierre Auger Observatory, can suffer from overcounting due to inclined muons generating signals in two adjacent segments. This effect, known as "corner clipping", introduces a bias in the muon estimator that increases with the zenith angle. To correct for this, the common approach is to parameterize the bias as a function of the zenith and azimuth angles using air-shower and full-detector simulations. This correction, which relies entirely on simulations, is then applied to the data. In this work, we introduce a data-driven method to quantify and correct the corner-clipping effect. Although we use the UMD of the Pierre Auger Observatory as an example, this procedure can be applied to any segmented detector with time resolution.

The 7th International Symposium On Ultra High Energy Cosmic Rays
(UHECR2024)
17 – 21 November, 2024
Malargüe, Mendoza, Argentina

*Speaker

PoS(UHECR2024)078

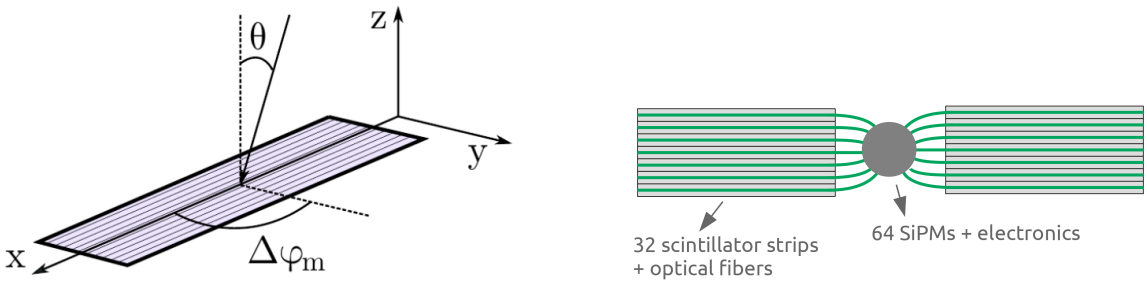

Figure 1: *Left*: Geometry of the shower as seen by a UMD module. θ corresponds to the zenith angle and $\Delta\phi$ is the azimuth angle of the shower measured relative to the azimuth orientation of the detector. *Right*: Sketch of a UMD module with its two halves.

1. Introduction

The Underground Muon Detector (UMD) of the Pierre Auger Observatory consists of an array of plastic scintillator muon counters, each of which is buried at a depth of 2.3 m in the vicinity of a water-Cherenkov detector. The soil shields the detector from non-muonic particles and imposes an energy cut of ∼1 GeV for vertical muons. Each UMD station comprises three modules of 10 m^2 of plastic scintillator. In turn, a module is segmented into 64 strips, with embedded wavelength-shifting optical fibers coupled to an array of 64 silicon photomultipliers (SiPMs). A sketch of a UMD module is shown in the right panel of Fig. 1.

In the binary mode of the UMD, each SiPM output is handled by a dedicated channel with a sampling time of 3.125 ns, generating a binary trace with 2048 samples. For each sample, a '1' is recorded if the SiPM signal — after electronic processing — exceeds a discriminator threshold; otherwise, a '0' is recorded. Muon signals within each bar are identified as a sequence of four or more consecutive '1's, referred to as a muon pattern. The activation number, k, which represents the number of bars presenting a muon pattern in an air-shower event, is the main observable used to estimate the number of muons in each detector (see Ref. [1] for details).

The observable k is influenced by several factors — common to any segmented detector — which, if not taken into account, can bias its interpretation. These factors include pile-up, corner clipping, detector inefficiency, and noise. Pile-up occurs when two or more muons hit the same scintillation bar within the time resolution of a detector, causing them to be recorded as a single muon, leading to undercounting. Corner-clipping muons are inclined muons that can produce signals in two adjacent bars, resulting in overcounting. This effect can occur when the muon itself traverses neighboring segments or when a deviating knock-on electron activates the neighboring bar of the primary muon. We note that this is a geometry-dependent effect, increasing with the zenith angle and becoming more pronounced in detectors whose azimuth is more perpendicular to the shower axis (see left panel of Fig. 1). Detector inefficiency (a muon failing to activate any bar) and noise (spurious muon patterns caused by spontaneous light emission in the scintillator-fiber system) are sub-dominant and contribute only negligibly [2].

The pile-up effect was extensively studied in Refs. [3–6] under the assumption of an ideal segmented detector with no corner-clipping muons. In this idealized scenario, probability distributions for k and pile-up-robust muon estimators were derived. To apply this formalism to data, the bias

introduced into this estimator by corner-clipping muons had to be parameterized as a function of the zenith and azimuth angles of the shower using full detector simulations. This simulation-based correction was then applied to the data. This approach was employed to analyze the first data from the engineering array of the UMD [7].

In this work, we present a novel method to quantify and correct the corner-clipping effect in a data-driven manner. This involves introducing a new data-driven quantity: the single-muon corner-clipping probability, p_{cc}. In Section 2, we describe the method to estimate this quantity. In Section 3, we show how this quantity is integrated into the reconstruction procedure and demonstrate its effectiveness in correcting the corner-clipping bias.

2. Data-driven method to estimate p_{cc}

It is first necessary to consider the detector in terms of halves, as they are the most irreducible units of material in which a particle can be injected (see right panel of Fig. 1). In addition, we will denote the number of activated bars in one half as $\tilde{k}$. Thus, the total number of triggered bars in a module can be written as $k = \tilde{k}_1 + \tilde{k}_2$, where $\tilde{k}_1$ and $\tilde{k}_2$ correspond to the number of triggered bars in half 1 and 2, respectively.

When a single muon is injected into a half, three outcomes are possible: no bar is activated ($\tilde{k} = 0$), a single bar is activated ($\tilde{k} = 1$) or two neighboring bars are activated ($\tilde{k} = 2$). If we call $N_{1\mu}$ the number of times in which only a single muon was injected into a half, we can write

$$N_{1\mu} = N_0 + N_{1\text{-bar}} + N_{\mathrm{cc}}, \tag{1}$$

where N_0, $N_{1\text{-bar}}$, and N_{cc} are the number of times in which zero, one, and two (neighboring) bars were activated, respectively. Thus, we can define the *single-muon corner-clipping probability* as

$$p_{\mathrm{cc}} = \frac{N_{\mathrm{cc}}}{N_{1\mu}}. \tag{2}$$

If we neglect detector inefficiency, which is a reasonable assumption given the large detection efficiency measured with a single bar [2], we can approximate $N_{1\mu} \cong N_{1\text{-bar}} + N_{\mathrm{cc}}$. Therefore, we have

$$p_{\mathrm{cc}}(\theta, \Delta\phi) = \frac{N_{\mathrm{cc}}(\theta, \Delta\phi)}{N_{1\text{-bar}}(\theta, \Delta\phi) + N_{\mathrm{cc}}(\theta, \Delta\phi)}, \tag{3}$$

where we explicitly indicate the dependence with θ and $\Delta\phi$. This quantity formally depends on θ_μ and $\Delta\phi_\mu$, the zenith and azimuth angles of the muon, but since these are not directly accessible in a real air-shower event, we approximate the direction of the muon using the direction of the shower, considering that muons are highly collimated. Since counting the number of module halves with only one activated bar is straightforward, estimating p_{cc} reduces to estimating N_{cc}.

We begin by considering the number of UMD module halves with only two activated bars (i.e. $\tilde{k} = 2$), which we call $N_{2\text{-bars}}$:

$$N_{2\text{-bars}} = N_{\mathrm{neigh}} + N_{\text{non-neigh}}, \tag{4}$$

where N_{neigh} and $N_{\text{non-neigh}}$ are the number of halves in which the two bars were neighboring and non-neighboring, respectively. Further, we can write

$$N_{\mathrm{neigh}} = N_{\mathrm{cc}} + N_{2\mu}, \tag{5}$$

where $N_{2\mu}$ is the number of times in which the neighboring pair of bars were activated due to two different muons. Thus, determining $N_{\rm cc}$ requires a method to distinguish whether neighboring bars are activated by a corner-clipping muon or by two separate muons. For that purpose, the timing information of the signals can be exploited.

We define Δt as the absolute difference between the start times of the two signals involved, where the start time corresponds to the instant of the first '1' in the muon pattern. In Fig. 2, we show the histograms of the Δt values for halves with $\tilde{k} = 2$ for a set of simulated showers (left) and data (right). The former consists of a library of CORSIKA [8] showers with energies E of $10^{17.5}$, 10^{18}, and $10^{18.5}$ eV and zenith angles θ of 0, 12, 22, 32, 38, and 48 degrees. Proton and iron are used as primary particle species, and EPOS-LHC [9, 10] is employed as the hadronic model. The detector simulation was performed by Offline, the official software to simulate and analyze data of the Observatory [11]. We separate the neighboring and the non-neighboring case into two different histograms. Both for data and simulations, it is apparent that the neighboring histogram shows a distinctive peak for small Δt that is not present in the non-neighboring case. For simulations, we further split the neighboring case into two categories: the corner-clipping case (green-filled histogram), obtained by requesting a single muon injected, and the two-muon case (grey-filled histogram). In the corner-clipping case, both signals are generated by the same muon almost simultaneously, within the limits of the detector resolution. As shown in Fig. 2, the corner-clipping events are concentrated in the range $\Delta t/(3.125\text{ ns}) \lesssim 5$. Very few additional entries for $\Delta t/(3.125\text{ ns}) > 5$ are visible in the green-filled histogram caused by the rare activation of a neighboring bar due to a non-muonic uncorrelated particle. We conclude that the Δt distribution of the neighboring case is the sum of two distributions: one peaked at small Δt values generated by corner-clipping muons (green-filled histogram), and the other caused by two different muons randomly hitting two neighboring bars (grey-filled histogram). Furthermore, we expect the two-muon case to have the same Δt distribution as the non-neighboring case as they both correspond to the same underlying process, namely, two muons randomly hitting two different bars. Thus, any statistically significant deviation between the time distributions of the neighboring and non-neighboring cases can be solely attributed to the corner-clipping muons. We use this to estimate $N_{\rm cc}$.

Given the condition that two (and only two) out of 32 bars are activated, the probability of them being neighboring just by chance can be shown to be $p_{2\mu}^{\rm exp} = 6.45\%$. The subindex 2μ is to emphasize that this situation corresponds to two different muons that randomly hit two neighboring bars and the supraindex is to indicate that this is an expected value using only a probabilistic consideration. Therefore, in the absence of corner-clipping muons (i.e., sufficiently large Δt), we expect $\frac{N_{\rm neigh}}{N_{\rm neigh}+N_{\text{non-neigh}}}$, the neighboring fraction, to be compatible with 6.45%.

In Fig. 3, the neighboring fraction is displayed for each Δt for simulations (left) and data (right), computed by dividing the blue histogram by the sum of the blue and orange histograms in Fig. 2 for each Δt bin. The dashed-grey line corresponds to $p_{2\mu}^{\rm exp}$, while the dotted-magenta line indicates $p_{2\mu}^{\rm meas}$, calculated as the neighboring fraction using only pairs of strips with $\Delta t/(3.125\text{ ns}) > 6$. It is apparent that, in this regime, the neighboring fraction remains constant and that $p_{2\mu}^{\rm meas}$ and $p_{2\mu}^{\rm exp}$ are consistent.

In contrast, for $\Delta t/(3.125\text{ ns}) < 6$, a rapid increase in the neighboring fraction is observed as a consequence of the corner-clipping effect. In this regime, for each Δt, we can estimate the number

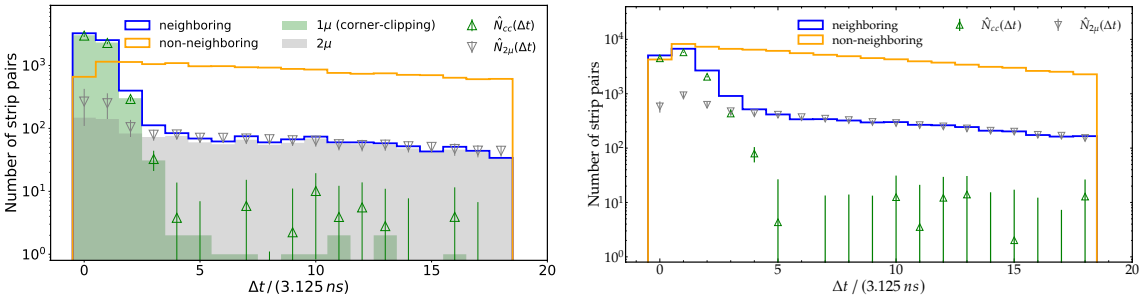

Figure 2: Distribution of Δt for UMD-module halves with only two bars with a muon pattern (i.e. $\tilde{k} = 2$) for simulations (left) and data (right). The non-neighboring case is represented by an unfilled-orange histogram, while the neighboring case is shown as an unfilled-blue histogram. For simulations, the neighboring case is divided into the cases in which one (green-filled histogram) or two muons (grey-filled histogram) were injected. The grey and green triangular markers correspond to the estimators of Eq. (6) and Eq. (7), respectively.

of pairs that correspond to the two-muon case as

$$\hat{N}_{2\mu} = p_{2\mu} \left(N_{\text{neigh}} + N_{\text{non-neigh}} \right) . \tag{6}$$

Therefore, an estimate for N_{cc} is obtained by replacing $\hat{N}_{2\mu}$ in Eq. (5):

$$\hat{N}_{cc}(\Delta t) = N_{\text{neigh}}(\Delta t) - \hat{N}_{2\mu}(\Delta t) = N_{\text{neigh}}(\Delta t) - p_{2\mu} \left(N_{\text{neigh}}(\Delta t) + N_{\text{non-neigh}}(\Delta t) \right) , \tag{7}$$

where we have explicitly indicated that the equation holds for each Δt.

In Fig. 2, the estimations obtained by Eq. (6) (grey-empty markers) and Eq. (7) (green-empty markers) are displayed for each Δt, both for data (right) and simulations (left). A high degree of agreement between the estimations and the true histograms can be seen, as observed in the simulations.

In order to get an estimate of the total number of corner-clipping muons, as needed in Eq. (3), we sum over all $\Delta t/(3.125 \text{ ns}) \leq 5$:

$$\hat{N}_{\text{cc}}^{\text{tot}} = \sum_{\Delta t=0}^{5} \hat{N}_{\text{cc}}(\Delta t).$$

Thus, an estimator $\hat{p}_{\text{cc}}$ can be constructed by replacing N_{cc} by $\hat{N}_{\text{cc}}^{\text{tot}}$ in Eq. (3). By applying this procedure in bins of $(\theta, \Delta\phi)$, the angular dependence of $\hat{p}_{\text{cc}}$ can be obtained. For data, we use the $(\theta, \Delta\phi)$ values retrieved from the surface detector reconstruction [12]. The results are shown in Fig. 4 for simulations (left) and data (right). The same qualitative behavior is observed in both cases, with the values for simulations being slightly larger than those for data, particularly at the most inclined zenith angles, suggesting that the corner-clipping effect may be overestimated in the simulations. As expected, $\hat{p}_{\text{cc}}$ increases with θ, and for a fixed θ, it increases as $\Delta\phi$ approaches 90° (or equivalently, as $|\sin(\Delta\phi)|$ approaches 1). This result represents the first observation and quantification of the corner-clipping effect in data.

For a fixed θ, we fit

$$p_{\text{cc}}(\theta, \Delta\phi) = m(\theta) \left(|\sin \Delta\phi| - \frac{1}{2} \right) + b(\theta). \tag{8}$$

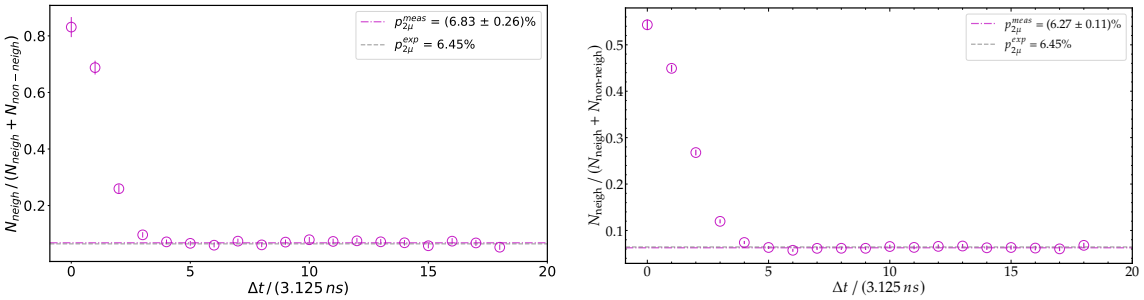

Figure 3: Fraction of neighboring pairs for each Δt for simulations (left) and data (right), obtained by dividing the neighboring histogram by the sum of the neighboring and non-neighboring histograms of Fig. 2. Grey-dashed line represents the expected value of the fraction in the absence of corner-clipping muons. Magenta-dashed line corresponds to the neighboring fraction using only pairs with $\Delta t/(3.125\text{ ns}) > 6$.

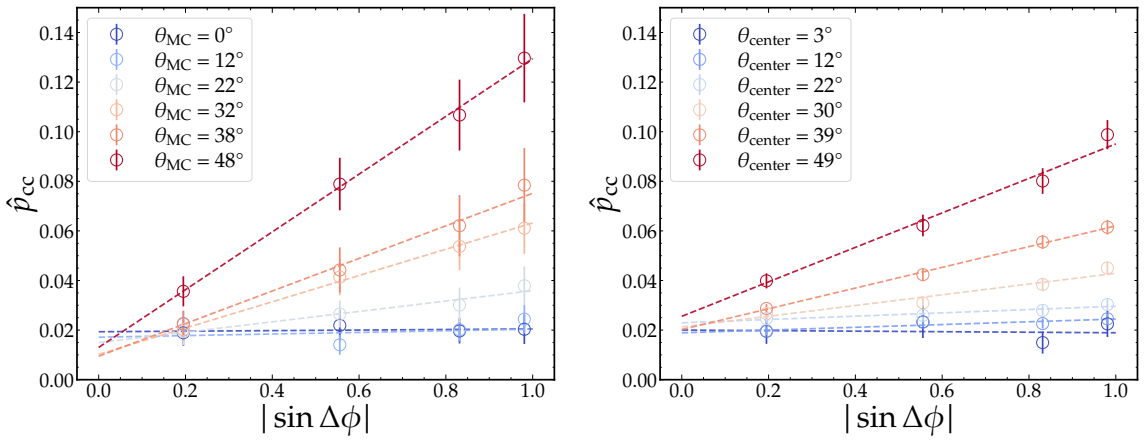

Figure 4: Estimated single-muon corner-clipping probability for simulations (left) and data (right). The dashed lines indicate the fits to Eq. (8). For data, the center of the zenith angle bin is indicated in the legend.

In turn, we fit m and b with with linear functions in $\sec\theta$.

The simulations can be used to assess the bias of $\hat{p}_{cc}$ by comparing it to the true p_{cc}. The true p_{cc}, calculated via Eq. (2) using the true values of N_{cc} and $N_{1\mu}$, is compared to the estimated $\hat{p}_{cc}$ in Fig. 5. It is clear that the proposed method offers an effective estimator of the corner-clipping probability.

3. Integrating p_{cc} to the reconstruction

In the previous section, we derived an unbiased method to estimate the probability of a single muon producing overcounting by activating two neighboring bars, p_{cc}. In this section, we explain how this quantity can be used to correct for this effect.

Assuming that (i) the number of muons in a detector follows a Poisson distribution with expected value μ and (ii) each muon can activate only one strip (i.e., no corner-clipping), a probability distribution of the activation number k can be derived [4]. This distribution, by construction, accounts for the possibility of pile-up (i.e., two muons hitting the same strip), but it does not model

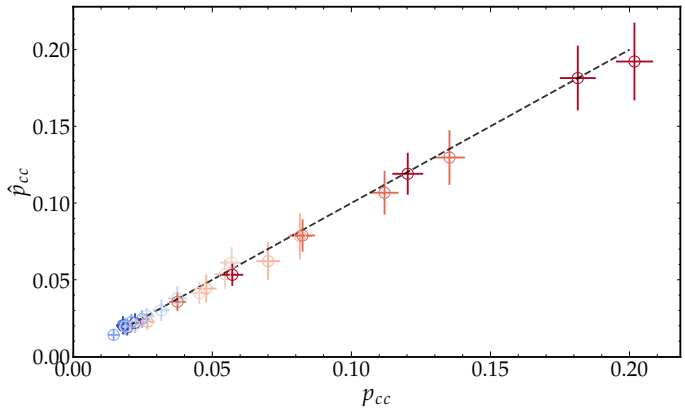

Figure 5: Comparison between estimated and true corner-clipping probability with simulations. The different marker colors indicate different zenith angles, following the same color convention as in Fig. 4. The dashed line indicates the identity function.

the corner-clipping effect. It is relevant to note that, actually, pile-up and corner clipping are related, since a strip activated by a corner-clipping muon may also be hit by a different muon during the event. In other words, corner-clipping signals can pile up with other single-muon signals. As a result, the overall effect of corner clipping is to increase the number of effective particles. If μ is the expected number of muons in a detector, then $\mu p_{\rm cc}$ represents the expected number of corner-clipping muons. Therefore, we propose substituting μ with an increased effective number of expected particles, $\mu(1 + p_{\rm cc})$, in the distribution of k, which now reads

$$P(k|\mu) = \binom{64}{k} e^{-\mu(1+p_{\rm cc})} \left(e^{\mu(1+p_{\rm cc})/64} - 1\right)^k . \tag{9}$$

For a measured k, Eq. (9) represents the likelihood of a detector. Maximizing Eq. (9) with respect to μ, the maximum likelihood estimator for the number of muons, now accounting for corner-clipping muons, reads

$$\hat{\mu} = \frac{-64}{1 + p_{\rm cc}} \ln(1 - k/64). \tag{10}$$

To assess if the parameter $\hat{p}_{\rm cc}$ retrieved by the method is useful to correct for the corner-clipping bias, we evaluate the bias of the estimator of Eq. (10) using simulations, where the parameterization of $\hat{p}_{\rm cc}$ shown in the left panel of Fig. 4 is used.

The mean relative bias of the estimator of Eq. (10) over detectors in the range $100 \leq r/\mathrm{m} \leq 1000$ as a function of θ for both primaries and all energies is shown in Fig. 6. It is evident that the uncorrected estimator (Eq. (10) with $p_{\rm cc} = 0$) shows an increasing bias with θ, while the corrected one shows a flat bias of less than 3%. We conclude that $\hat{p}_{\rm cc}$ successfully captures the behavior of the bias caused by corner-clipping muons with the zenith angle.

4. Summary and outlook

We have developed a novel data-driven method to correct the bias introduced by corner-clipping muons in the Underground Muon Detector of the Pierre Auger Observatory. This method is also

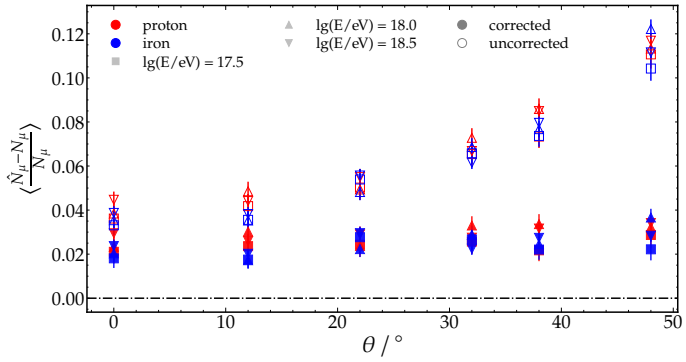

Figure 6: Mean relative bias of the estimator of Eq. (10) over detectors in the range $100 \leq r/\mathrm{m} \leq 1000$ as a function of θ. The shape of the different markers correspond to different energies, while different colors indicate different primaries. The full markers correspond to the corner-clipping-corrected estimator, whereas empty markers indicate the uncorrected estimator (Eq. (10) with $p_{\mathrm{cc}} = 0$).

generally applicable to any segmented detector with time resolution. It estimates the single-muon corner-clipping probability, p_{cc}, by analyzing timing distributions between signals in adjacent bars and comparing them to those from non-neighboring signals in detector halves with only two activated bars. This approach enables the corner-clipping effect to be measured and characterized using data for the first time.

Simulations demonstrate that p_{cc} effectively captures the bias caused by corner-clipping muons, allowing for its use to correct for this effect in data. In this way, the corner-clipping bias, previously addressed solely through simulations, can now be accounted for in a data-driven way, minimizing the influence of detector simulations in the data analysis.

We are currently working on extending the method to detector halves with more than two activated segments, which will allow us to apply the method with greater statistical power.

References

[1] J. de Jesús for the Pierre Auger Collaboration, *PoS* **UHECR2024** (2024) 077
[2] The Pierre Auger Collaboration, JINST **16** (2021) P04003.
[3] A. D. Supanitsky et. al., Astropart. Phys. **29** (2008) 461-470.
[4] Ravignani, D. and Supanitsky, A. D., Astropart. Phys. **65** (2015) 1–10.
[5] A.D. Supanitsky, Astropart. Phys. **127** (2021) 102535.
[6] F. Gesualdi and A. D. Supanitsky, Eur. Phys. J. C **82** (2022) P925.
[7] The Pierre Auger Collaboration, Eur. Phys. J. C **80** (2020) 1-19.
[8] D. Heck *et al.*, Report FZKA **6019** (1998).
[9] K. Werner *et al.*, *Phys. Rev. C* **74** (2006) 044902.
[10] T. Pierog *et al.*, *Phy. Rev. C* **92** (2015) 034906.
[11] S. Argiro et al., Nucl. Instrum. Meth. A **580** (2007) 1485.
[12] The Pierre Auger Collaboration, JINST **15** (2020) P10021.